

Periodic forcing in a three level cellular automata model for a vector transmitted disease

L. B. L. Santos, M. C. Costa, S. T. R. Pinho,* and R. F. S. Andrade
Instituto de Física, Universidade Federal da Bahia, 40210-340, Salvador, Brazil

F. R. Barreto, M. G. Teixeira, and M. L. Barreto
Instituto de Saúde Coletiva, Universidade Federal da Bahia, 40110-140, Salvador, Brazil
 (Dated: November 9, 2018)

The transmission of vector infectious diseases, which produces complex spatiotemporal patterns, is analyzed by a periodically forced two-dimensional cellular automata model. The system, which comprises three population levels, is introduced to describe complex features of the dynamics of the vector transmitted dengue epidemics, known to be very sensitive to seasonal variables. The three coupled levels represent the human, the adult and immature vector populations. The dynamics includes external seasonality forcing (rainfall intensity data), human and mosquito mobility, and vector control effects. The model parameters, even if bounded to well defined intervals obtained from reported data, can be selected to reproduce specific epidemic outbursts. In the current study, explicit results are obtained by comparison with actual data retrieved from the time-series of dengue epidemics in two cities in Brazil. The results show fluctuations that are not captured by mean-field models. It also reveals the qualitative behavior of the spatiotemporal patterns of the epidemics. In the extreme situation of absence of external periodic drive, the model predicts completely distinct long time evolution. The model is robust in the sense that it is able to reproduce the time series of dengue epidemics of different cities, provided the forcing term takes into account the local rainfall modulation. Finally, the dependence between epidemics threshold and vector control undergoes a transition from power law to stretched exponential behavior due to human mobility effect.

PACS numbers: 87.18.-h, 87.16.aj, 87.19.xd, 87.15.A

I. INTRODUCTION

Understanding the rather complex dynamics of transmissible diseases is of utmost importance for improving life quality, and even the survival of some human population groups. To achieve this, interdisciplinary efforts are necessary, which certainly include the use of the recently techniques developed to study complex systems [1, 2, 3]. At the beginning of 21 century, both directly transmitted diseases, like tuberculosis and AIDS, as well as vector-transmitted diseases, such as dengue and malaria, are still not controlled. In modern life, the intense flux of people at global level and within large cities [4] increases the complexity of the propagation of transmitted diseases [5]. For vector-transmitted diseases, there are already indications that climatic conditions and vector mobility may increase the number of cases [6]. In the case of dengue, an arboviral disease transmitted to humans by *Aedes* mosquitoes (mainly *Aedes Aegypti*), several determinant factors for its transmission are found in large urban centers [7]: human concentration, large inter- and intra-city human mobility, the climatic conditions for the vector proliferation (high humidity and temperature between $15^{\circ}C$ and $40^{\circ}C$). Accordingly, it is found that the dengue outbursts are quite sensitive to seasonal varia-

tions in pluviometric precipitations, humidity and temperature. The disease, which may be caused by four different virus serotype (DenV1-DenV4), reaches yearly some 50 millions people in more than 60 countries, with ~ 21000 casualties [8].

Since 1992 [9], ordinary differential equation (ODE) models have been proposed to analyze dengue inter-host dynamics and the effect of vector control actions. More recently, some attempts to introduce the spatial dependence on the disease propagation have been reported, using both partial differential equation (PDE) [10] and cellular automata (CA)[11] models, and other data analysis techniques [12]. In [11], the authors proposes a model that takes into account only the description of mosquito population, which may be found in the adult phase, and the immature phase comprising several stages. However, a more accurate description of the dengue propagation must include, besides the interaction among these population groups, the vector mobility, effect of control actions, and an explicit climatic periodic forcing on the population variables. To our knowledge, no previous investigation has taken into account all of these factors.

In this work, we investigate an inter-host three level CA model, which describe the pertinent population groups in a urban environment: human, adult vector mosquito, and immature vector in the aquatic phase. As we will detail later on, it includes all of the quoted effects: external forcing to describe the environment influence on the vector life cycle, as well as other interaction terms de-

*Corresponding author, email: suani@ufba.br

scribe the effect of human and vector mobility and control actions. The results provided by the model reproduce actual time series from some well document dengue epidemics in specific years urban centers in Brazil. Besides that, they also qualitatively agree with main features of the spatiotemporal patterns. We also show that, in the absence of a periodic forcing, the actual epidemic outbursts are not reproduced, supporting the claims of the importance of climatic aspects in the triggering of local events. Finally, as the model describes the behavior of the exposed population for larger time intervals under the presence of climatic seasonal variations, it is possible to follow the effect of vector control actions. In such case, our results indicate a power law dependence between the epidemic threshold and the parameter describing the intensity of vector control.

The current description of vector-transmitted diseases goes along several successful works based on CA intra-host disease propagation models (for instance, AIDS, [13], malaria [14], cancer [15]) and also on inter-host models [16]. It is also worth mentioning that the presence of multiple CA interacting levels in epidemic models has been explored in alternative topologies, as that of complex networks where nodes represent patches of regular lattices [17] submitted to a contact process dynamics [18].

The paper is organized as follows: in Section II, we introduce the CA local rules, comparing them to other models in the literature. Section III discusses the choice of parameter values in our simulations. In Section IV, we present our results, comparing them with actual data: the simulated time series (IV A) resulting from the periodic forcing seasonal effects, the simulated spatiotemporal patterns and the vector control associated to human mobility effect. Finally, Section V closes the paper with concluding remarks and perspectives.

II. THE MODEL

Some of the basic interaction mechanisms and external effects be included in our three level CA model have been used, in other context, by previous ODE models reported in the literature. The first attempt [9] considered a compartment model, in which humans follow SEIR (susceptible, exposed, infected and removed) dynamics. Since mosquitoes usually die before being removed, the authors consider that they follow a simpler three-compartment SEI version. On the other hand, climatic effects were modeled by seasonal variations of model parameters by an ODE system [19]. Tuning models by comparison to actual data have also been attempted, e.g., by the estimation of the basal transmission rate for age-stratified data from Thailand [20]. Other models have considered the role of a unique vector in the transmission of multiple diseases, as more than one dengue serotype [21, 23, 24] or the concurrent transmission of yellow fever in dengue infested areas [25]. Finally, the effect of vector control have already been explicitly analyzed in ODE models

[23, 24, 26].

Each of three CA levels consists of a two-dimensional square lattice with $N_s = L \times L$ sites. Correspondingly, the CA is subjected to closed boundary conditions because it mimics dengue transmission in a city. If we compare the results to actual data, each neighborhood corresponds to a set of distinct spatial units (census sectors) into which the reported cases are assigned to. Each site in the distinct levels describe, respectively, the local populations: human (H), mosquito (M) and immature vector in the aquatic phase (A). The CA inter-layer interaction rules couple, locally, the three involved levels due to the interactions between H and M levels, and the A to M flux of the vector population. The CA Moore neighborhood with radius 1 allows, for each site of a given layer, a maximum of 9 neighbors in the level it interacts with (see Figure 1). We restrict ourselves to the one-serotype situation, although the model can be extended to simulate the dynamics with more than one serotype.

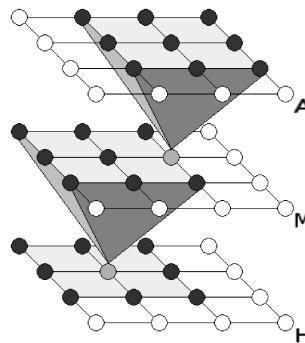


FIG. 1: Diagram of different lattices: humans (H), mosquitoes (M) and aquatic phase (A). Note that each element of lattices H and A ‘sees’ up to nine neighbors of the lattice M (and vice-versa).

According to previously indicated models, in the A phase, the vector is found in one of 4 compartments: egg (E), larvae (L), pupae (P) and breeding (B). The M phase comprises 3 compartments: susceptible (SM), exposed (EM), and infectious (IM). Finally, considering only one serotype, there are 4 possible compartments for H sites: susceptible (SH), exposed (EH), infectious (IH), and recovered (RH). Moreover, sites of A and M levels can be in empty states, denoted by EAS and EMS . The local interaction rules, based on the entomological [27] and epidemiological aspects [28], are such that, for each level: (see Figure 2).

A level: E , L , P and B states evolve from the preceding one after the E eclosion period t_e , L phase period t_l and P phase period t_p . An empty site EIM may be replaced with probability $f_s(t)$ by an E state, if there is at least an occupied site in its Moore neighborhood at the M level. The transition from E to L compartments also depends on $f_s(t)$, much as the persistence of B , which releases

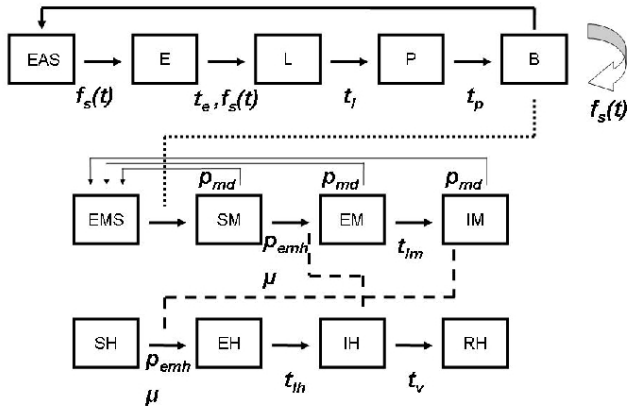


FIG. 2: A schematic representation of the local rules of the model.

an adult mosquito SM to a EPM site of the M level.

M level: The population in the M level results from the dynamics in A phase. Adult population M dies according to a death probability p_{dm} in any state. The transition from a SM site into EM depends on the number of IH sites in its neighborhood in the H level, on the local effective biting humans-mosquitoes probability p_{ehm} , and on the human mobility μ . An EM site becomes IM after the M virus latent period t_{lm} .

H level: In a similar way to the $SM \rightarrow EM$ transition, a SH site changes to EH according to the local effective mosquitoes-humans biting probability (p_{emh}), the number of IM sites in the M level neighborhood, and on the human mobility μ . EH becomes infectious IH after the H virus latent period t_{lh} , and IH becomes recovered RH after the viremia period t_v .

Note that, in the above level descriptions, we already included relevant features of dengue transmission that we have called the attention in Section 1. Seasonal information (rainfall intensity) is used as input data [6] [7] by tuning the time dependence of the $f_s(t)$ probability, using a Fourier expansion of the actual rainfall series. If the time series do not include daily entries, or is not complete over the whole simulation period, interpolation or addition of random noise to the day average taken over a few years can be used. Global infection probabilities between H and M populations, due to mobility in private and public transport systems, is described by a global (mean-field) mobility parameter μ . The action of

μ , which is the same for all sites, is to globally increase the $SM \rightarrow EM$ and $SH \rightarrow EH$ probability transitions, without any influence from the neighborhood population in the other level.

Finally, the decrease of populations in M level resulting from vector control actions is included by the following additional rule: the natural M death probability is increased by an additional amount p_{adm} , which reduces the adult mosquitoes on any state of the M level.

III. PARAMETER VALUES

The CA parameters introduced in the previous section can be classified into four classes, according to the individual process they describe: 1) Spatial parameters, as L and μ ; 2) Temporal parameters: t_e , t_l , t_p , t_{lm} , t_v , and t_{lh} ; 3) The probabilities of transmission and mosquito death parameters: p_{emh} , p_{ehm} , and p_{md} ; 4) Vector control parameter: p_{adm} .

The values of spatial parameters are obtained by taking into account the data of a given urban center. We estimate the size L of the lattice (number of sites = L^2) by the area of the city (A_c) and the flight radius of the vector (R). More specifically, we assume that $A_c = L^2 a$, where a is the area of one cell, while R corresponds to the average (*Moore*) neighborhood radius. This way, we have

$$R = \frac{\sqrt{a}(1 + \sqrt{2})}{2} \implies L = \sqrt{\frac{A_c}{a}} = \frac{\sqrt{A_c}(1 + \sqrt{2})}{2R} \quad (1)$$

As the dispersion of *Aedes aegypti* due to its flight rarely exceeds $100m$ [33], we assume $R = 100m$. The range of values of μ was estimated by requiring that the model reproduces the same behavior of the histogram of the number of census sectors with, at least, one reported dengue case during the corresponding time period.

We assumed fixed values (within the range presented in Table I) for the probabilities of transmission $p_{ehm} = p_{emh} = 0.75$ [9] and of mosquito death $p_{md} = 1/7 = 0.143$. For vector control parameter, when is the case, we scrutinize the complete interval from 0 to 1.

Choosing the CA iteration time unit to be one day, we are able to set value intervals for several temporal parameters according to the literature (see Table I). To obtain baseline values for temporal parameters and epidemic threshold, we adapt the epidemiological definition of an epidemic process [34] to our model simulations. A disease is considered epidemics if the annual incidence I , the number of reported case to susceptible population, is above a certain (epidemics) threshold I_{th} . Therefore, I_{th} may be given by

$$I_{th} = \langle I \rangle + 2\sigma, \quad (2)$$

where the average incidence $\langle I \rangle$ is calculated with respect to the last N years and σ corresponds to the

standard deviation. To obtain corresponding model values, we run the program for N different random seeds. We recall that, as for actual cases of vector transmitted diseases, several numerical simulations resulting from different random seeds die out in the first weeks, being characterized as small endemic processes.

After the evaluation of $\langle I \rangle$ and σ , we run the program as many times as necessary to get K independent samples with $I > I_{th}$. Although we perform the numerical simulations of the model for large time intervals, our analysis can be restricted to 364 time unit intervals if we want to compare the results with actual data of one year epidemics series. The output data are the time series of density of each state in the H , M and A levels of the CA model, and the spatiotemporal configurations at any time step. The cpu time increases according to L^3 and linearly with the number of samples.

Finally, based on the range of values in Table I for temporal parameters, simulations have been conducted for an initial set of parameter values. Then, we investigate the effect of changing one by one parameter, while holding all the others fixed. This way, we identify the baseline values that minimizes the error between the actual time series and the simulated time series. We perform several tests in order to check the robustness of the chosen initial set of parameter values. For a systematic analysis of parameter values, we considered an average of M simulations samples, identifying the best output for the purpose of comparison with one actual epidemics time series. This is achieved by the analysis of the minimum discrepancy between actual and simulated time series:

$$e = \frac{\sum_{i=1}^T |a_i - s_i|}{T}, \quad (3)$$

where T is the number of days, a_i is the actual incidence and s_i is the simulated incidence of day i .

Once estimated the baseline of temporal parameter values, the analysis of minimal discrepancy is also applied to select the best sample in comparison to actual data.

IV. RESULTS

In order to validate the model, we consider the data of the first dengue epidemics (DenV-2) in 1995, Salvador, Brazil [35], when its population $p_c = 2.3$ million habitants distributed over an $A_c = 313 \times 10^6 m^2$ area. In 1995, the average daily temperature was $25.89^\circ C$ with 1.47 standard deviation. The city yearly mean precipitation is 1980 mm/year, while seasonal effects concentrate precipitation in the months March-August.

A. The seasonal effects: actual and simulated time series

The 1995 weekly rain intensity Γ_R and reported number of new dengue cases I_D (incidence) are shown in Figure 3, where the data have been normalized by the largest input for the sake of comparing the tendency of the curves. As, in this case, temperature and humidity are quite stable, rainfall is the most important climatical factor for dengue propagation. Indeed, the Pearson correlation varies from 0.49 to 0.76 for, respectively, weekly and monthly sampled data. As it will be clear from the discussion of our results, such increase in the correlation in value is due to a roughly two week delay time between the two signals. When the series are clustered in large time windows, such effects become much smaller. The daily rainfall data was provided by the Brazilian government [36].

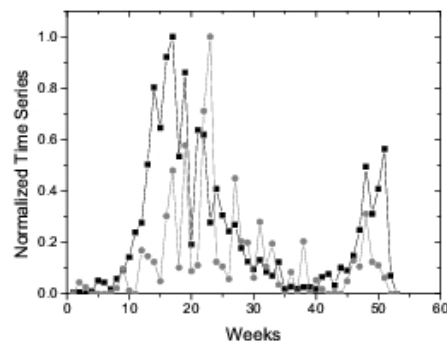


FIG. 3: Normalized time series of weekly I_D in Salvador (black-squares) and normalized time series of weekly Γ_R (grey-circles) for 1995. The normalization factor are 846 cases and 373 mm respectively.

The simulations are based on the function $f_s(t)$ corresponds to the Fourier expansion

$$f_s(t) = a_0 + \sum_{j=1}^{12} a_j \cos(\pi jt/26) + b_j \sin(\pi jt/26) \quad (4)$$

with $a_0 = 0.13585$, $a_1 = -0.12872$, $b_1 = 0.05071$, $a_2 = 0.0502$, $b_2 = -0.0882$, $a_{12} = 0.00744$, $b_{12} = 0.04713$. The total contribution of the the remaining coefficients a_i, b_i can be neglected.

The 10,831 reported dengue cases in Salvador during 1995 were geo-referenced by epidemiological week (52 temporal units) and census sectors (2600 spatial units)[35]. Note that, due to large official sub-notifications (26 %), the actual number of cases is much larger. In Salvador, the epidemics peak occurs before the rainfall peak, what can be justified by the fact that, due to the high intense pluviometric precipitation peak,

the rainfall washes out the vector in the immature phase. As well will see later, this may not happen in other urban centers. According to expression (1), we are lead to the value $L = 214$. On the other hand, the value $\mu = 5 \times 10^{-4}$, has been selected from the interval where the model is able to reproduce the exponential behavior in the probability distribution of observed new cases in a year among 2600 sensus sectors (not shown).

Assuming that there is one infected individual in each site of H lattice, the best sample is able to reproduce the actual data quite well, as shown by the normalized actual and simulated incidence time series in Figure 4. We normalize both the actual and simulated time series for the purpose of avoiding distortions due to large sub-notifications. To set up the correspondence between I_R and the simulated incidence IH_N , that is, the number of new infected humans at a time step, we use the scale factor L^2/p_C . The normalization factors for the actual and the best simulated incidence time series result, respectively 17 and 11.

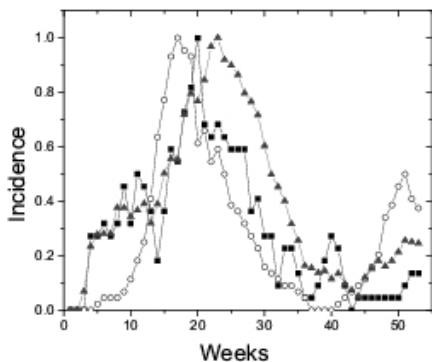


FIG. 4: Actual (I_D) and simulated (IH_N) weekly incidence time series of Salvador in 1995 normalized by largest single input. The data has been smoothed by averaging on three consecutive weeks. Circles, squares and triangles indicate, respectively, I_D , the best individual sample, and average value over 20 samples taken from random seeds. The normalization factors for I_D , the best IH_N and the averaged IH_N , are 17, 11 and 14 respectively. Consider one sample and the following parameter values: $t_e = 5$, $t_i = 5$, $t_p = 3$, $t_{lm} = 7$, $t_{lh} = 6$, $t_v = 6$, $p_{ehm} = p_{emh} = 0.75$, $p_{md} = 0.143$, $\mu = 5 \times 10^{-4}$.

Note that the delay between the peaks of I_D and the best individual sample is much smaller than the delay between Γ_R and I_D in Figure 3, even considering the averaging on three consecutive weeks which amplify the delay effect. Although this effect is also amplified for the average over some samples, it is still smaller than the delay between I_D and Γ_R in Figure 3.

To emphasize the importance of the periodic forcing to recover the reported I_D values, we draw, in Figure 5, the time evolution according to two hypothetical scenarios.

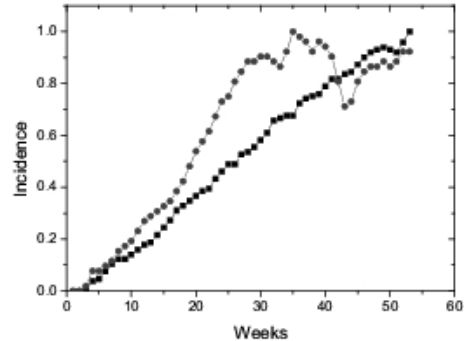


FIG. 5: Normalized average over 20 samples of simulated weekly incidence (IH_N) when $f_s(t) = 1$ (black square) and $f_s(t) = \sin(2\pi t/52)$ (grey circle). The normalization factors for $f_s(t) = 1$ and $f_s(t) = \sin(2\pi t/52)$ are 35.5 and 17.3 respectively. The data has been smoothed by averaging on three consecutive weeks. Parameter values are the same as in Figure 4.

They were obtained by replacing $f_s(t)$, in first place, by a constant value, and afterwards by a simple periodic sine function. The resulting incidence counts differ substantially from the typical patterns in Figure 5. The importance of such external drive, which is a crucial aspect of vector transmitted diseases, has been neglected in most of analyzed models with time and space dependence.

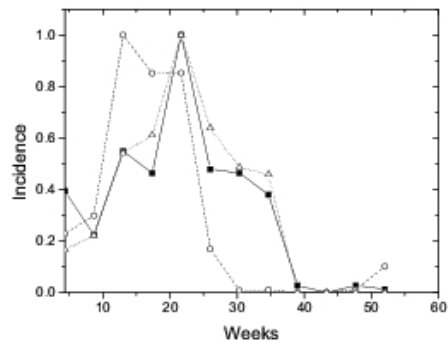


FIG. 6: The normalized rain intensity (Γ_R), actual (I_D) and simulated (IH_N) incidence (by month) in Mossoró in 1999. The normalization factors are 71 cases, 149.5 mm, and 72 cases respectively. Consider the best sample and the following parameter values: $t_e = 4$, $t_i = 7$, $t_p = 7$, $t_{lm} = 6$, $t_{lh} = 5$, $t_v = 6$, $p_{ehm} = p_{emh} = 0.75$, $p_{md} = 0.143$, $\mu = 1.0 \times 10^{-6}$. The used lines-symbols are, respectively, dashed white-circle, solid black-square, and dotted grey-triangle.

The importance of seasonal aspects for the observed dynamics can be further exemplified by running the

model with the data of other urban centers. For instance, we consider the 1999 dengue epidemics in Mossoró, in Northeast Brazil [38], for which rainfall peak precedes Γ_R the reported incidence I_D peak. In this case, for which only monthly data are available for both incidence and rainfall, not only the rainfall regime is different from that in Salvador, but also notice a smaller Pearson's correlation coefficient ($c=0.69$) between rainfall and dengue incidence (see Figure 6).

Mossoró's larger surface of $A_c = 2110 \times 10^6$ m [39] directly influences spatial parameters, leading to a lattice size $L = 554$. As this incidence data is not georeferenced, μ could not be directly estimated. However, taking into account that the city is a less developed urban center with a smaller population than Salvador ($p_c = 234.390$ habitants [39]), we consider a smaller value of $\mu = 1.0 \times 10^{-6}$. The values of other parameters were chosen according to the already discussed procedures. We observe that the normalization factors for the actual (71) and the simulated (72) incidence time series are very similar. The results in Figures 4 and 6 show that the model is robust enough to simulate dengue incidence for cities with high and low rain intensities, and different Pearson correlation coefficients. Thus, such results indicates that, besides the importance of periodic forcing, the epidemic behavior of vector transmitted diseases are heavily dependent on entomological and epidemiological aspects that are also caught by the model.

To better understand the forcing effect, the behavior of CA model has been followed for large time intervals. We consider that the exactly the same rainfall incidence obtained from one-year pluviometric data is repeated periodically [12]. Our results indicate that the periodic forcing leads to modulated responses. However, if we disallow the possibility of new exogenous infected sources (due, e.g., to an infected visitor), the amplitude of the epidemic outbursts does not remain the same. If the same parameter values as in Figure 4 are used, the results in Figure 7 indicate that IH_N oscillation amplitude reaches its maximum value in the second year, when it starts decreasing in a steady way. It is interesting to note that, at the same time, the M and A populations do not decrease in a similar way. This indicates that, in a closed environment, the number of individuals carrying active virus and a relatively weak screening effect due to a small RH population, turns it difficult to trigger new epidemic events. Note that, after five years, the number of susceptible individuals SH in the population is still very high: 97% for the parameter set that causes the incidence go to zero.

On the other hand, Figure 7 also shows that changes in the parameter values, favoring virus permanence in M and H levels for a longer time, may lead to the opposite landscape, with a long period during which the yearly amplitude of IH_N population increases monotonically. In such cases, the amplitude decreases only when a large fraction of the H population has become infected and switched to the RH state. Note that this is not yet

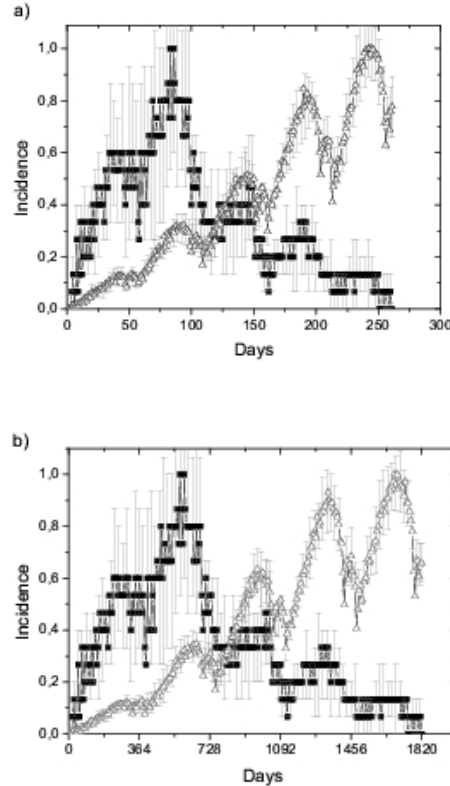


FIG. 7: Predicted average IH_N for a large time interval of 5 years as function of entomological features. a) Different values of probability of mosquito death: black squares and dark-grey triangles indicate, respectively, $p_{md} = 1/7 = 0.143$ and $p_{md} = 1/8 = 0.125$, while the corresponding normalization factors are 15 and 202. b) Different values of human viremia period: black squares and dark-grey triangles indicate, respectively, $t_v = 5$ and $t_v = 7$, with normalization factors 15 and 219. Other parameter values are the same as in Figure 4. Averages and respective error bars (grey) have been taken over $M_{samples} = 20$.

the situation, after 5 years evolution period, for such alternative time evolution scenarios. There we still find a large fraction of SH susceptible individuals: 52% (see Figure 7a), where we introduce a variation of probability of mosquito death that is the inverse of expected life time of mosquito ($p_{md} = 1/8 = 0.125$), and 46% (see Figure 7b) where the variation occurs in the human viremia ($t_v = 7$). The different values of normalized factors in both cases indicate how these parameters increases the number of IH_N .

This dramatic dependence of the size of successive epidemic events in isolated environments turns to to be a unexpected result of our model. As far as we know, this effect, resulting from a local interaction between the three CA levels, has not been previously discussed in the literature.

B. The mobility effects: spatiotemporal patterns and vector control

Spatiotemporal patterns resulting from geo-referenced data of the actual epidemics of Salvador in 1995 have been reported elsewhere [35]. They can be compared to the CA simulated spatiotemporal patterns, which have been generated with the help of the G2 graphic package [37]. To this purpose, it is necessary to assume that, in each CA level, more than one individual can live in each lattice site. We consider that the total population of the city is represented by the CA cells, assuming the inhabitants are a gaussian distributed among the cells with a mean value of 50 humans per cell. With this assumption, the model is able to reproduce qualitatively the main features observed in actual spatiotemporal epidemics patterns [35].

In Figure 8, we illustrate spatiotemporal patterns for A , M and H populations in characteristic time steps. For the sake of a better visualization, we choose a small value of lattice size ($L = 79$). As initial condition, we assume an infection seed, represented by one IH site in the H level. Further, due to a previous large rainfall event, the E and SM states of the A and M levels are largely populated. From this time on, epidemics starts around the site where the seed was located. SM changes into EM state, disseminating the disease into other H sites, while increasing the radius of the primary epicenter. Due to H and M mobility, some secondary epicenters are formed. In this case, without any control strategy, the epidemics evolves naturally until its end. Figure 8 reveals qualitative similarities to the main features presented in [35]: the persistence of the epicenter of the epidemics, the emergence of secondary epicenters, and an irregular shape of each epicenter.

Secondary epicenters at large distances from the original seed are a direct consequence of the mobility effects, which are well accepted to be an important feature for dengue transmission urban centers. Indeed, if $\mu = 0$, the shown spatiotemporal pattern is replaced by a diffusion-like pattern with a single epicenter. However, μ also plays an important role in reducing time series fluctuations, an expected ‘mean-field’ effect related to the global infection probability. This effect is made clear in Figure 9. The curves also show that non-zero values of μ introduce a time delay effect extending the duration and the intensity of the epidemics process. Indeed, the large difference in the normalization factors for both curves indicates that μ is directly related to a much faster epidemic dissemination.

Until today, no efficient vaccine against dengue could be devised. Therefore, actions towards vector control constitute the only public health policy to reduce the deleterious effect of the disease. Even so, there are still controversies regarding whether vector control actions are more reliable in the A or M phases. As the CA model is able to successfully reproduce epidemics data and follow the dynamics of the disease for longer periods

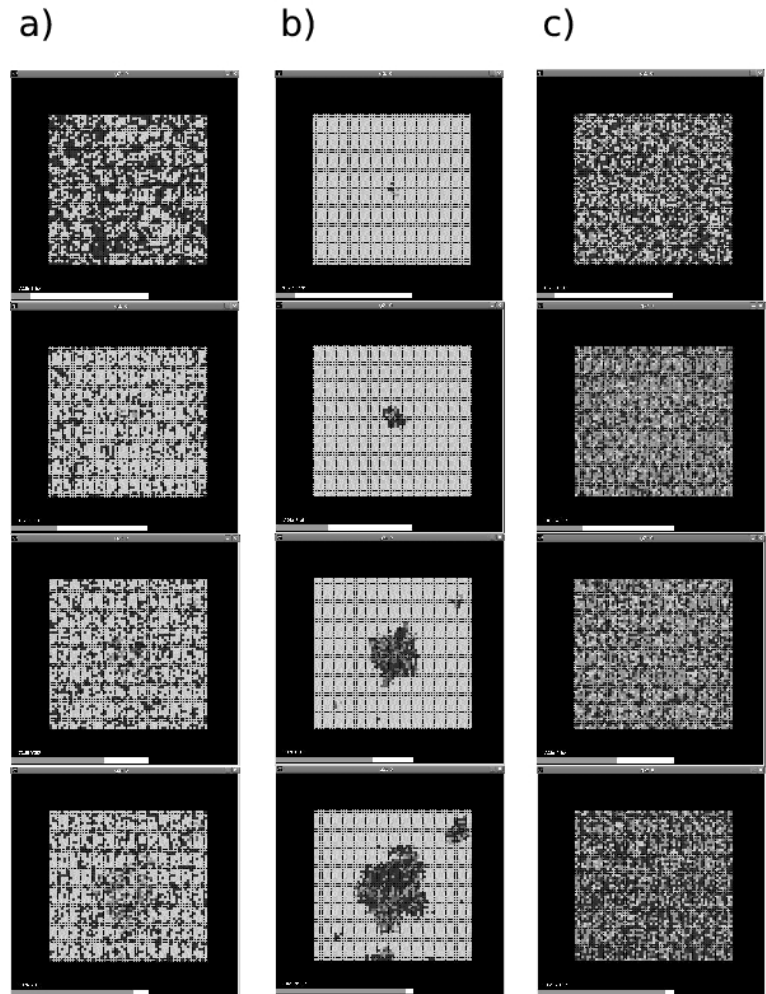


FIG. 8: Simulated spatiotemporal configurations of cumulated cases, consider one sample and the following parameter values: $L = 79$, $p_{md} = 0.143$, $p_{emh} = p_{ehm} = 0.75$, $\mu = 0.001$, $t_e = 5$, $t_l = 7$, $t_p = 3$, $t_m = 7$, $t_{lh} = 5$, $t_v = 5$. Four snapshots for each lattice: a) Mosquitoes (M); b) Humans (H); and c) Aquatic phase (A). For on line version: ((M): empty site - blue, SM - green, EM - grey, IM - red), ((H): SH - green, EH - grey, IH - red, RH - blue), ((A): empty site - blue, E - green, L/P - grey, B - red). For printed version: ((M): empty site - white, SM - light-grey, EM - dark-grey, IM - black), ((H): SH - white, EH - light-grey, IH - dark-grey, RH - black), ((A): empty site - white, E - light-grey, L/P - dark-grey, B - black)

of time, it can also provide useful insights regarding the effect produced by different vector control mechanisms.

To this purpose, let us consider the dependence between the epidemic threshold and the vector control parameter p_{amd} . We have performed a large number of independent simulations for different values of p_{amd} . We evaluated I_{th} with the help of equation (2), where the

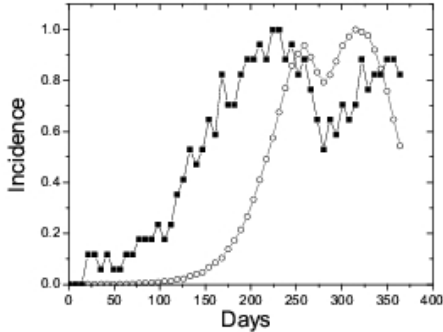


FIG. 9: The mobility parameter effect: normalized IH_N assuming $M_{samples} = 200$ and the same parameters values of figure 4 except μ that is assumed the following values: 0.0 (black square) and 0.02 (white circle). The normalization factors are, respectively, 17 and 1867.

time average was replaced by sample averages. Thus, I_{th} is directly related to the probability that an individual living in the simulated urban center gets infected within a one-year time span.

The results in Figure 10 show that, when $\mu = 0$, the dependence between I_{th} and p_{amd} follow a power law behavior, $I_{th} = ap_{amd}^\alpha$, with large values. It clearly shows that effective policies aiming at a reduction of the vector reproduction in its own environment produce substantial reduction of affected population. This effect is still more expressive and relevant when we consider more realistic situations, in which human and vector population move in the urban space. Indeed, when $\mu > 0$, I_{th} decays with respect to p_{amd} in a faster way the points of fit quite well to a stretched exponential $I_{th} = b_1 \exp[-b_2(p_{amd}^\beta)]$. Moreover, as expected, the epidemic threshold is larger, for any value of p_{amd} , when $\mu > 0$ than when $\mu = 0$.

V. CONCLUDING REMARKS AND PERSPECTIVES

The three level CA model investigated in this work presents several features that allow for a quantitative reproduction of actual time series of dengue epidemics. Besides the usual local interaction steps based on SEIR compartment models, the most important novelties are: i) the use of the climatological data as input data; ii) the $A - M$ and $M - H$ inter-level interactions; iii) the inclusion of short-range vector mobility and long-range human mobility.

The model is robust with respect to the range of parameters considered in the literature, and to its ability in reproducing time series of dengue epidemics in different urban centers. The climatic input data as well as the procedure used for estimating the parameter values

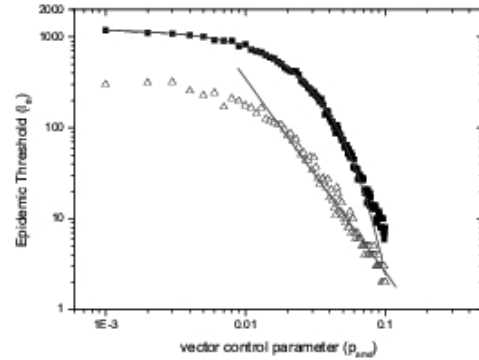


FIG. 10: The vector control analysis: the simulated $I_{th} \times$ vector control parameter (p_{amd}). We consider $M_{samples} = 20$ and the same parameters values of Figure 4, except for the parameter $\mu = 0$ and $\mu = 10^{-5}$. The corresponding values are indicated by, respectively, white triangles and black squares. The parameters of the power law fitting (grey), for $\mu = 0$, is the exponent $\alpha = -2.13 \pm 0.04$ and $a = -1.72 \pm 0.05$. The parameters of the stretched exponential fitting (grey), for $\mu = 10^{-5}$, are $b_1 = 1218.04 \pm 7.00$, $b_2 = 86.44 \pm 4.00$, and the exponent $\beta = 1.14 \pm 0.01$.

are able to catch the diversity of the time series dengue incidence for different cities. Although we have mainly focused our analysis on the human population, the CA model also provides useful insights on the behavior of the vector population, which will be presented in a future work.

The effect of periodic forcing allows us to suggest effective measures to reduce the probability of recurrent outbreaks. Indeed, the effect of an increased infected vector life time is found to be very important to alter of the magnitude of epidemic events.

The analysis of vector control shows that, as expected, it indeed produces a decrease in the probability of human infection. However, we have shown that this effect is more relevant when vector and human mobility are taken into account. In this case, the infection probability decreases according to an stretched exponential, while a power law behavior is observed when the no mobility assumption is taken into account.

Perspectives for further work on this model are of two kind. The first one amounts to investigate the impact of different strategies of vector control on dengue transmission as well as to discuss the detailed behavior of M and A populations subject to those strategies. A more ambitious goal is to achieve the quantitative reproduction of spatial patterns. This requires a more precise local characterization of spatial units, as well as a more precise GPS georeferencing data. This way, the CA model can help to plan improved vector control policies from the spatial point of view, attacking mainly the most important focus for the propagation of the epidemics.

Acknowledgements: The authors thank C. P. Ferreira, D. Alves, E. Massad, H. M. Yang, J. G. V. Miranda, J. P. Dias, L. Esteva, M. N. Burattini, V. C. G. S.

Morato for useful discussions about dengue modeling. The authors acknowledge the Brazilian agencies CNPq and FAPESB for financial support.

-
- [1] N. Boccarda, *Modeling Complex Systems Series: Graduate Texts in Contemporary Physics* (Springer Verlag, New York, 2004).
- [2] P. Philippe, *Nonlinear Dynamics, Psychology, and Life Sciences* **4**, 275-295 (2000).
- [3] R. Anderson, and R. May, *Infectious Diseases of Humans - Dynamics and Control* (Oxford University Press, Oxford, 1991).
- [4] G. Chowell, J. M. Hyman, S. Eubank, and C. Castillo-Chavez, *Phys. Rev. E* **68**, 066102 (2003).
- [5] D. J. Gubler, *Dengue and dengue hemorrhagic fever: its history and resurgence as a global health problem*. In: Gubler, D.J.; Kuno, G.; editors. *Dengue and dengue hemorrhagic fever*. New York: CAB International, 1-22 (1997).
- [6] S. Hales, N. de Wet, J. Maindonald, and A. Woodward, *The Lancet* **360**, 830 (2002).
- [7] G. Kuno, *Epidemiologic Reviews* **17**, 321 (1995).
- [8] World Health Organization. <http://www.who.int/mediacentre/factsheets/fs117/en/> accessed at July 5, 2008.
- [9] E. A. C. Newton, and P. Reiter, *Am. J. Trop. Med. Hyg.* **47**, 709 (1992).
- [10] N. A. Maidana, and H. M. Yang, *TEMA Tend. Mat. Apl. Comput.* **1**, 83 (2007).
- [11] H. M. Yang, and C. P. Ferreira, *App. Math. and Comput.* **111**, 1i(2007).
- [12] A. Vecchio, L. Primavera, and V. Carbone, *Phys. Rev. E* **73**, 031913 (2006).
- [13] R. M. Zorzenon dos Santos, and S. G. Coutinho, *Phys. Rev. Lett.* **87**, 16810 (2001).
- [14] R. M. Zorzenon dos Santos, S. T. R. Pinho, C. P. Ferreira, and P. C. A. da Silva, *The Eur. Phys. J. ST* **1**, 125 (2007)
- [15] E. A. Reis, L. B. L. Santos, and S. T. R. Pinho *A cellular automata model for avascular solid tumor growth under therapy action*, e-print:arXiv:0806.1063.
- [16] A. Johansen, *J. theor. Biol.*, **178**, 45 (1996).
- [17] S. L. Silva, J. A. Ferreira, and M. L. Martins, *Physica. A* **377**, 689 (2007).
- [18] S. C. Ferreira, and M. L. Martins, *Phys. Rev. E* **76**, 036112 (2007).
- [19] F. A. B. Coutinho, M. N. Burattini, L. F. Lopez, E. Massad, *Bull. Math. Biol.* **68**, 2263 (2006).
- [20] N. M. Ferguson, C. A. Donnelly, and R. M. Anderson, *Phil. Trans. R. Soc. London B* **354**, 757(1999b).
- [21] L. Esteva, and C. Vargas, *J. Math. Biol.* **46**, 31 (2003).
- [22] H. M. Yang, and C. P. Ferreira, *Appl. Math. Comput.* **198**, 401 (2008).
- [23] L. M. Bartley, C. A. Donnelly, and G. P. Garnett, *Trans. R. Soc. Trop. Med. Hyg.* **96**, 387 (2002).
- [24] I. B. Schwartz, L. B. Shaw, D. A. T. Cummings, L. Billings, M. McCrary, and D. S. Burke, *Phys. Rev. E* **72**, 066201 (2005).
- [25] E. Massad, F. A. B. Coutinho, M. N. Burattini, and L. F. Lopez, *Trans. R. Soc. Trop. Med. Hyg.* **95**, 370 (2001).
- [26] L. Esteva, and H. M. Yang, *Math. Biosc.* **198**, 132 (2005).
- [27] N. A. Honrio, W. C. Silva, P. J. Leite, J. M. Goncalves, L. P. Lounibos, and R. Loureno-de-Oliveira, *Mem. Inst. Oswaldo Cruz* **98**, n.2, Rio de Janeiro Mar. 2003.
- [28] M. G. Teixeira, M. C. N. Costa, M. L. Barreto, and L. E. Mota, *Cadernos de Saúde Pública (FIOCRUZ)* **21**, 1307 (2005).
- [29] J. F. Siler, M. H. Hall, and A. P. Hitchens, *Philipp. J. Sci.* **29**, 1 (1926).
- [30] D. J. Gubler, W. Suharyono, R. Tan, M. Abidin, A. Sie, *Bull. W. H. O.* **59**, 623 (1981).
- [31] L. Rosen, L. F. Rozeboom, D. J. Gubler, J. C. Kien, B. N. Chianotis, *Am. J. Trop. Med. Hyg.* **34**, 603 (1985).
- [32] P. M. Sheppard, W. W. MacDonald, R. J. Tonn, and B. Grab, *J. Animal Biol.* **38**, 661 (1969).
- [33] C. Liew, and C. F. Curtis, *Med. Veter. Entomol.* **18**, 351 (2004).
- [34] D. P. Barker, and F. J. Bennett, *Practical of epidemiology* (Churchill, Livingstone, 1976).
- [35] F. R. Barreto, M. G. Teixeira, M. C. N. Costa, M. S. Carvalho, and M. L. Barreto, doi:10.1186/1471-2458-8-51, *BMC Public Health* **8**, 51 (2008).
- [36] (Ministério da Agricultura e do Abastecimento - Instituto Nacional de Meteorologia INMET 4º Distrito).
- [37] Lj. Milanovic, and H. Wagner, g2 - graphic library (C) 1999 (<http://g2.sourceforge.net>)
- [38] J. P. Dias, *Avaliação da efetividade do Programa de Eradicação do Aedes aegypti. Brasil, 1996-2002*, PhD Thesis, Universidade Federal da Bahia, Brazil (2006).
- [39] BRASIL. Instituto Brasileiro de Geografia e Estatística (IBGE). <http://www.ibge.gov.br/home/> accessed at July 8, 2008.

| <i>Parameter</i> | <i>Range of values</i> |
|---------------------------------------------------------------------|------------------------|
| Egg period (t_e) [27] | 4-5 days |
| Larvae phase period (t_l) [27] | 5-7 days |
| Pupae phase period (t_p) [27] | 2-3 days |
| Latent period of virus in the mosquito (t_{lm}) [9, 22, 27, 29] | 7-20 days |
| Latent period of virus in the human (t_{lh}) [9, 22, 29] | 2-12 days |
| Viremia period (t_v) [9, 22, 30] | 3-7 days |
| Probability of transmission human-mosquito (p_{ehm}) [31] | 0.5-1.0 |
| Probability of transmission mosquito-human (p_{emh}) [9] | 0.5-1.0 |
| Probability of mosquito death (p_{md}) [9, 25, 32] | 0.128-0.25 |

TABLE I: The parameter range of values of temporal parameters and the probabilities of transmission H-M and M-H, and of death mosquito according to the literature. The baseline values were chosen for the simulations of the model.